Optimizing the conditions for hydrothermal liquefaction of barley straw for bio-crude oil production using response surface methodology

Zhu, Zhe; Rosendahl, Lasse Aistrup; Toor, Saqib Sohail; Chen, Guanyi

Published in:
Science of the Total Environment

DOI (link to publication from Publisher):
10.1016/j.scitotenv.2018.02.194

Creative Commons License
Unspecified

Publication date:
2018

Document Version
Accepted author manuscript, peer reviewed version

Optimizing the conditions for hydrothermal liquefaction of barley straw for bio-crude oil production using response surface methodology

Zhe Zhu[a], Lasse Rosendahl[b], Saqib Sohail Toor[b], Guanyi Chen[c]

[a]School of Environmental Science and Safe Engineering, Tianjin University of Technology, Tianjin, 300384, PR China

[b]Department of Energy Technology, Aalborg University, Aalborg, 9220, Denmark

[c] School of Environmental Science and Engineering/State Key Laboratory of Engines, Tianjin University, Tianjin, 300072, PR China

Abstract:

The present paper examines the conversion of barley straw to bio-crude oil (BO) via hydrothermal liquefaction. Response surface methodology based on central composite design (CCD) was utilized to optimize the conditions of four independent variables including reaction temperature (factor X_1, 260-340 °C), reaction time (factor X_2, 5-25 min), catalyst dosage (factor X_3, 2-18 %) and biomass/water ratio (factor X_4, 9-21 %) for BO yield. It was found that reaction temperature, catalyst dosage and biomass/water ratio had more remarkable influence than reaction time on BO yield by analysis of variance (ANOVA). The predicted BO yield by the second order polynomial model was in good agreement with experimental results. A maximum BO yield of 38.72 wt% was obtained at 304.8 °C, 15.5 min, 11.7 % potassium carbonate as catalyst and 18% biomass (based on water). GC/MS analysis revealed that the major BO components included phenols and their derivatives, acids, aromatic hydrocarbon, ketones, N-contained compounds and alcohols, which makes it a promising material in the applications of either as a phenol substitute in bio-phenolic resins or bio-fuel.

Key words: Hydrothermal liquefaction, Barley straw, Central composite design, Response surface methodology

1. Introduction

Nowadays, issues related to energy security, climate change mitigation, and sustainable development enhanced the overall utilization of renewable energy, which is the world's fast-growing energy source. Among them, bioenergy is the largest

renewable energy source worldwide, the total supply of which accounted for 10.3% of the global energy supply in 2014. (Kummamuru, 2017). Barley straw, an agricultural residue, represents one of the largest lignocellulosic biomass in Denmark. In 2016, almost 2.17 million tons of barley straw was produced. Unfortunately, 34.12% was left on the field and has not been utilized yet. Only 22.56% was converted to energy through combustion and power generation etc., 29.74% was used as fodder (Denmark, 2014). Therefore, there is an urgency to find suitable solutions to convert remaining straw. One of the effective methods for crops straw utilization is biofuel production through fast pyrolysis (Das and Sarmah, 2015; Hsieh et al., 2015; Xu et al., 2017) and hydrothermal liquefaction (HTL) (Gollakota et al., 2017; Midgett et al., 2012; Younas et al., 2017), which is anticipated to provide 27% of global transportation fuels by 2050. Most importantly, it is estimated that for OECD countries 2.1 Gton of carbon dioxide in the atmosphere can be reduced every year according to such use of biofuels (IEA, 2012).

HTL has gained significant interest in recent years, and has been demonstrated to be competitive with thermochemical routes such as pyrolysis for converting biomass into biofuels due to feedstock flexibility, high energy and resource efficiency of the process and high output product quality (Patel et al., 2016; Suárez-Iglesias et al., 2017). Feedstock flexibility and process efficiency are important factors for the sustainable operation of new biofuel technologies. HTL converts diversified biomass in hot compressed liquid (water/organic solvent) into four different products: bio-crude oil (BO) with higher heating values up to 38 MJ/kg (Toor et al., 2011), aqueous phase containing multiple organic compounds which can be reused in this process (Déniel et al., 2016; Hu et al., 2017; Zhu et al., 2015a) or utilized for cultivation of microalgae afterwards (Hu et al., 2017), solid residues used for heating or as soil amendment (Yu et al., 2017), as well as gaseous products mainly including CO_2 and H_2. In particular, bio-crude oil, a promising alternative energy source with high energy density, has the potential to be used as a liquid fuel in boilers, engines and turbines or chemical feedstocks (Xiu and Shahbazi, 2012). Therefore, HTL of barley straw with emphasis on bio-crude production was conducted in this study.

Production of BO from barley straw using HTL technology has been investigated in our previous studies (Zhu et al., 2015a; Zhu et al., 2015b; Zhu et al., 2014) where the single-factor experiments were conducted, and product yield and properties were studied as well. It showed that the maximum BO yield of 34.9 wt% was achieved at 300 °C, 10 wt% K_2CO_3 as catalyst, biomass to water ratio of 15% under a fixed retention time of 15 min. In addition, low temperature (<320 °C) and with the addition of K_2CO_3 favor BO yield. Indeed, reaction time and biomass/water ratio influence the product distribution and properties as well (Toor et al., 2011). A number of independent factors were discussed, while the interactions between them were not considered. Therefore the conditions need to be further optimized.

Response surface methodology (RSM) is a kind of optimal design for regression model, which is a rapid technique for development, improvement and optimizing process, based on the data from experiments conducted at a set of input variables at multiple levels. It allowed established the significance of each parameter and the significant interaction between parameters. Compared with other experimental design methods, it has the advantage of optimizing nonlinear systems, providing a more precise computation of the main and interaction effects through regression fitting (Diamond, 1981; Eriksson et al., 1996; Hassan et al., 2017). Thus, this method has already been used to optimize process parameters during thermal conversion of different biomass, such as algae, cotton stalk, palm kernel shell etc. (Chan et al., 2017; Li et al., 2017; Liu et al., 2013). Li et al. (Li et al., 2017) optimized three operating parameters (microwave power, reaction temperature and time) during microwave-assisted pyrolysis. Chan et al. (Chan et al., 2017) performed optimization study on HTL of palm kernel shell using RSM with central composite rotation design (CCRD) involving four factors (temperature, pressure, reaction time and biomass to water ratio). Similarly, the CCRD was also employed by Liu et al. (Liu et al., 2013) to find the optimization conditions for HTL of macroalgae by three variables (temperature, catalyst and solvent/biomass ratio). Yet, little research has been conducted to investigate the bio-crude oil production from barley straw through HTL process.

This paper moves further to a more systematic study on the effects of four experimental variables (reaction temperature, reaction time, catalyst dosage, biomass/water mass ratio) and their interactions on bio-crude oil production based on the RSM experiment. A central composite design (CCD) experimental design was employed and the response surface model was analyzed. Finally, the validity of model was confirmed by conducting numerical examples. More detailed analysis of chemical properties of BO was performed, to provide a guidance for the design of utilization of barley straw and the further pilot and industrial scale practice.

2. Materials and Methods

2.1 Materials and characterization

The barley straw was obtained from Denmark. Before experiment, it was grounded into small particles having a size of less than 1.0 mm and then dried overnight at 105 ºC for 24 hours. The elemental composition is shown in Table 1. The elemental analysis (CHNS) of biomass was performed with a 2400 Series II CHNS/O Element analyzer (PerkinElmer, USA). The water content was determined by calculating the weight loss before and after drying at 105 ºC in an oven for at least 12 hours. Higher heating values (HHVs) were measured using C2000 basic Calorimeter (IKA, German).

Table 1 Elemental composition of raw biomass

Biomass	Elemental content (wt% dry basis)					HHV (MJ/kg)	Ash content (wt%)	Water content (wt%)
	C	H	N	S	O[a]			
Barley straw	44.66	6.34	0.46	0.57	47.97	17.38	4.26	6.21

[a] By difference

Typically, barley straw in Demark consists of cellulose, hemicellulose and lignin with the content of 46%, 23%, and 15%, respectively (Sander, 1997).

The reagent grade acetone was used as rinsing solvent for product separation, which was purchased from Sigma-Aldrich and used as received. Potassium carbonate (K_2CO_3) was purchased from Sigma-Aldrich and used as catalyst.

2.2 Experiment setup

The experiments were carried out in 10 mL micro reactors which were assembled by Swagelok tubes and fittings. The reactor consists of a 200 mm length of SS316 tube (12 mm O.D. with a wall thickness of 2 mm) fitted with a Swagelok cap at one end, and the other end was fitted with a capillary connected to a high pressure sensor. The real-temperature and pressure was transferred to the Matlab program through the data acquisition system. A fluidized baths (SBL-2D type with a TC-9D type temperature controller, Techne calibration) with maximum temperature of 600 ^{o}C was employed for heating reactors. Fig. 1 shows the schematic diagram of micro reactor. Prior to HTL experiments, we did pressure tests with nitrogen to make sure that the reactors were tightly sealed.

In a typical experiment, 6 g distilled water and between 0.54 and 1.26 g barley straw (making biomass concentration of 9-21wt% on a dry basis) was placed in the reactor, with a certain quantity of K_2CO_3 (2-18 wt% of biomass) as well. Then the reactor was sealed and purged with N_2 for three times to ensure that no air was remained inside. Before experiment, the reactors were pressured to 10 bars with N_2 in case of water boiling during heating. Then they were immersed in sand bath fluidized bed preheated to the set temperature and oscillated up and down which is controlled by VLT 2800 Variable-frequency drive. After the reactor reached to reaction temperature, it was hold at that temperature for the required time (5-25 min). Finally, the reactor was cooled down in cold water bath. For each of these conditions, the experiments were conducted in triplicates. The results herein are mean values, and uncertainties are standard deviations.

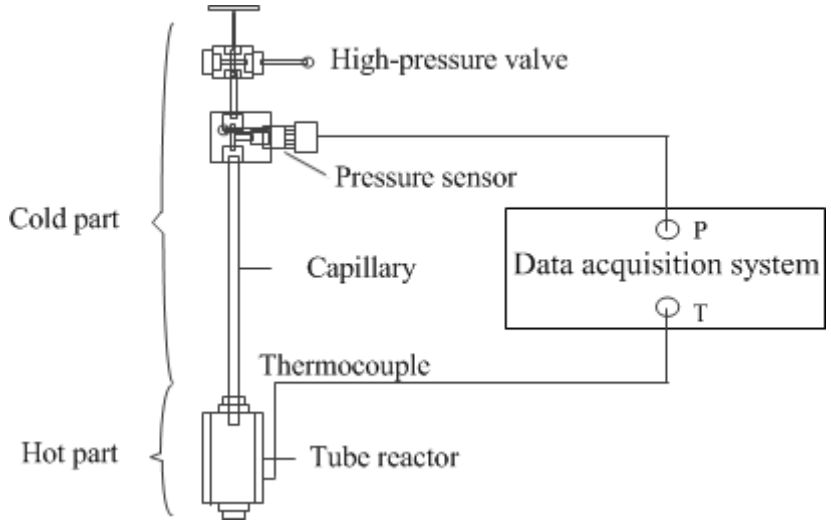

Fig. 1. Schematic diagram of micro reactor

2.3 Separation of reaction products

The cooled reactors were opened without collecting gaseous products. Since the main attention in this work was paid on the optimization of bio-crude oil production with higher yield and energy contents, gas fraction was thus not collected and analyzed in this work. Similar method was used in the literature (Déniel et al., 2016; Hu et al., 2017; Parsa et al., 2018; Zhang et al., 2009).

The liquid product was poured to a beaker and filtered through the Whatman No. 5 filter paper to separate the aqueous phase (AP) from solids. Then the reactor, cap and capillary were rinsed with acetone several times to remove any leftover matter including bio-crude oil and solids adhering on them. Afterwards, the mixture containing oil phase, solids and acetone were filtrated and the remaining solids on the filter paper were dried in a furnace at 105 ºC for 24 hours and then weighted to determine the solid residues (SR) yield. The acetone and water formed during HTL was removed by a rotary evaporator (Buchi Rotavapor R-210, Switzerland) at a reduced pressure at 60 ºC. The dark oil phase left was weighed and referred to as bio-crude oil (BO). The yieldS of BO and SR were determined on a dry basis by Eqs. (1-2):

$$BO\ yield\ (wt\%) = \frac{mass\ of\ BO\ obtained\ (g)}{mass\ of\ dried\ barley\ straw\ (g)} \times 100 \quad (1)$$

$$\text{SR } yield\ (wt\%) = \frac{mass\ of\ \text{SR}\ obtained\ (g)}{mass\ of\ dried\ barley\ straw\ (g)} \times 100 \quad (2)$$

2.4 Design of experiments

CCD is one of the most commonly used RSM designs for investigating the synergistic effect of different variables on a target parameter. In this study, the experimental design with 4 variables and 3 levels was employed to optimize the HTL of barley straw process conditions using Design Expert 9.0.3 software based on the response value (BO yield) obtained in the experiments. Four variables were reaction temperature (X_1), reaction time (X_2), catalyst dosage (X_3) and biomass/water mass ratio (X_4). Based on the preliminary single factor experiments(Zhu et al., 2015a; Zhu et al., 2015b; Zhu et al., 2014), the range of each value was chosen in the range of 260-340 °C, 5-25 min, 2-18 wt% and 9-21wt% respectively, as shown in Table 2. The design contained a total of 30 experiments, with 16 factorial design, 8 axial points, and 1 center point with 6 replicates to ensure the accuracy of the experiment. Herein, the factorial design was to estimate the curvature for the model. The center point offered a method for estimating the experimental errors and testing lack of fit.

The data was analyzed using Design Expert 9.0.3 and Minitab 18 software, optimizing the BO yield in this process. The analysis of variance (ANOVA) and significance test of the BO yield obtained under different operating conditions were carried out in order to evaluate the quality of the model fitting, while the residual analysis was performed to assess model adequacy. The quadratic polynomial equation was used to study the effects of the linear, square terms and interacting terms of the independent variables, as is shown is Eq. (3).

$$Y = a_0 + \sum_{i=1}^{4} a_i X_i + \sum_{i=1}^{4} a_{ii} X_i^{\,2} + \sum_{i=1}^{4} \sum_{i<j} a_{ij} X_i X_j \quad (3)$$

where Y is the response function (BO yield), X_1, X_2, X_3 and X_4 are the reaction temperature, reaction time, catalyst dosage and biomass/water mass ratio, respectively; a_0 is intercept of model, a_i, a_{ii}, a_{ij} represents the coefficients of linear, quadratic and interaction terms, respectively.

Table 2 Experimental variables and levles

	Variables	Level of variables				
		-2	-1	0	1	2
X_1	reaction temperature (°C)	260	280	300	320	340
X_2	reaction time (min)	5	10	15	20	25
X_3	catalyst dosage [a] (wt%)	2	6	10	14	18
X_4	biomass/water mass ratio (wt%)	9	12	15	18	21

[a] based on dry biomass

2.5 Characterization of BO

The elemental composition were determined using a 2400 Series II CHNS/O element analyzer (PerkinElemer, USA). Duplicate analysis of each element was conducted, and the mean value were presented here.

Higher heating values of BO were calculated according to Dulong formula, due to the fact that the BO collected in micro reactors was not enough for test.

$$\mathrm{HHV(MJ/kg)} = 0.3383\mathrm{C} + 1.422(\mathrm{H} - \mathrm{O}/8) \quad (4)$$

Where C, H, O represents the mass percentage of carbon, hydrogen and oxygen content, respectively.

The chemical composition of BO was analyzed on CLARUS SQ 8 Gas Chromatograph/Mass Spectrometer (GC/MS) from PerkinElmer. Before test, the samples were dried at 105 °C for 24 hours, and trimethylsilyl derivatization was applied so as to enhance the volatility of samples. The resulting silylated derivatives were diluted with 2.0 mL of hexane and subjected to a fixed temperature ramping profile: 75 °C (held 2 min) → 250 °C at a rate of 20 °C/min (held 10 min). The

compounds were identified using NIST 2011 spectrum library.

3. Results and Discussion

3.1 RSM results and response surface analysis

3.1.1 Model fitting

The experimental conditions and the response value (BO yield) are shown in Table 3. As shown in Table 3, the BO yield varied between 22.12 wt% and 37.64 wt% at different liquefaction conditions. The highest BO yield was obtained at a temperature of 300 ºC, 15min, with addition of 10% catalyst and biomass/water ratio of 21%. The fitting quadratic equation for BO yield is determined based on these data, as shown in Eq. (3).

$$Y = 34.9717 + 1.75X_1 + 0.286667X_2 + 1.42583X_3 + 1.65083X_4 - 0.4125X_1X_2 + 0.815X_1X_3 - 0.9325X_1X_4 - 0.23125X_2X_3 - 0.02625X_2X_4 - 0.25625X_3X_4 - 2.34X_1^2 - 0.29125X_2^2 - 1.5375X_3^2 - 0.53X_4^2 \quad (3)$$

The ANOVA was performed and the results are shown in Table 4. It was found that the model was highly significant with p-value <0.0001. The lower the p-value, the more significant the factor. Thus, the model was suitable for this experiment. In addition, the p-value of "lack of fit" was 0.0723 ($p > 0.05$), indicating that lack of fit was insignificant, which implied that the proposed model fit the data well. The quadratic polynomial regression model for BO yield showed that factor of X_1, X_3, X_4, the interaction term of X_1X_3, X_1X_4, and quadratic term of X_1^2, X_3^2 were significant, suggesting that the response was interactive and complicated. Besides, a high coefficient of determination value (R^2=0.9262) was obtained, which indicated that the model can predict the experimental data effectively.

227 **Table 3** CCD matrix, actual product yield and properties of BO

Run	variables				BO yield(wt%)	SR yield(wt%)	Elemental composition (wt%)				HHV(MJ/kg)
	reaction temperature(°C)	reaction time(min)	catalyst dosage (wt%)	biomass/water mass ratio (wt%)			C	H	N	O	
1	300	15	10	15	34.97±0.79	15.87±3.13	68.25	7.43	0.68	23.64	29.45
2	280	10	6	12	24.13±3.59	21.93±2.94					
3	320	20	14	18	33.99±2.18	18.91±1.21	69.21	7.21	0.71	22.87	29.60
4	320	10	6	12	28.85±1.59	12.75±2.41	67.94	6.89	0.75	24.42	28.44
5	300	15	10	15	34.97±0.79	15.87±3.13					
6	300	15	10	15	34.97±0.79	15.87±3.13					
7	300	5	10	15	32.78±2.56	17.86±1.98	68.08	7.13	0.78	24.01	28.90
8	320	20	6	12	27.88±1.59	15.12±1.85	68.78	7.45	0.73	23.04	29.77
9	300	15	18	15	32.62±1.59	17.27±1.76	67.27	6.84	0.73	25.16	28.01
10	280	10	14	12	26.14±0.85	24.97 ±2.11					
11	300	15	2	15	27.12±3.02	18.21±3.03	65.46	6.66	0.76	27.12	26.80
12	300	15	10	15	34.97±0.79	15.87±3.13					
13	280	20	6	12	25.14±1.24	23.18 ±1.64					
14	280	20	14	12	27.73±1.89	23.98 ±1.97					
15	280	20	14	18	29.97±0.97	24.99±2.43					

16	300	25	10	15	36.93±0.53	19.91±1.54	65.50	7.19	0.72	26.59	27.66
17	320	10	6	18	29.91±1.70	18.17±2.05	66.91	7.63	0.78	24.68	29.10
18	280	10	14	18	31.74±1.63	25.79±2.51					
19	300	15	10	15	34.97±0.79	15.87±3.13					
20	280	10	6	18	29.73±1.74	24.45±1.89					
21	320	20	14	12	31.83±2.17	18.45±2.72	67.98	7.96	0.72	23.34	30.17
22	320	10	14	18	34.24±0.58	18.71±2.68	68.28	7.19	0.69	23.84	29.09
23	300	15	10	9	30.16±0.93	17.38±2.49	67.92	7.53	0.91	23.64	29.48
24	300	15	10	15	34.97±0.79	15.87±3.13					
25	260	15	10	15	22.12±1.48	27.63±1.90					
26	320	10	14	12	33.96±0.94	14.31±2.79	67.36	7.12	0.67	24.85	28.50
27	320	20	6	18	29.25±1.66	18.25±2.84	68.14	7.23	0.75	23.88	29.09
28	340	15	10	15	31.20±1.83	19.12±3.13	69.31	7.33	0.72	22.64	29.85
29	300	15	10	21	37.64±0.69	17.26±2.99	68.83	7.09	0.82	23.26	29.23
30	280	20	6	18	31.49±1.77	28.34±1.09					

228 **Table 4** ANOVA of the RSM model for BO yield

Sources	Sum of squares	Degree of freedom	Mean square	F-value	P-value	Remarks
Model	410.77	14	29.34	13.45	<0.0001	Significant
X_1	73.50	1	73.50	33.69	<0.0001	Significant
X_2	1.97	1	1.97	0.90	0.3568	
X_3	48.79	1	48.79	22.36	0.0003	Significant
X_4	65.41	1	65.41	29.98	<0.0001	Significant
X_1X_2	2.72	1	2.72	1.25	0.2816	
X_1X_3	10.63	1	10.63	4.87	0.0433	Significant
X_1X_4	13.91	1	13.91	6.38	0.0233	Significant
X_2X_3	0.86	1	0.86	0.39	0.5406	
X_2X_4	0.011	1	0.011	5.053E-003	0.9443	
X_3X_4	1.05	1	1.05	0.48	0.4983	
X_1^2	150.19	1	150.19	68.83	<0.0001	Significant
X_2^2	2.23	1	2.23	1.07	0.3181	
X_3^2	64.84	1	64.84	29.72	<0.0001	Significant
X_4^2	7.70	1	7.70	3.53	0.0798	
Residual	32.73	15	2.18			
Lack of fit	29.03	10	2.90	3.92	0.0723	Not significant
Pure error	3.70	5	0.74			
Total	443.50	29				
R^2	0.9262					

229 **3.1.2 Diagnostics and validation of model**

230 To study the appropriateness of the model, the diagnostic plots such as normal
231 plot and predicted vs. actual were developed. Figs. 2-3 illustrate the normal
232 probability and residual plot of model for BO yield. The internally studentized
233 residual is calculated by the division of residual to its standard deviation, which is
234 used to estimate the error varying between points. Typically, each point on normal
235 probability plot should lie approximately in a straight line, thus it can be inferred that
236 the estimated effects are the real (Box and Draper, 2007). As observed in Fig. 2, the
237 plotted data formed a straight line roughly, so the residuals for BO yield fitted normal

distribution and the model was proved in good agreement with experimental data. In addition, the residual plot shown in Fig. 3 revealed that the residual of BO yield had a random scatter, therefore, no outlier points were detected.

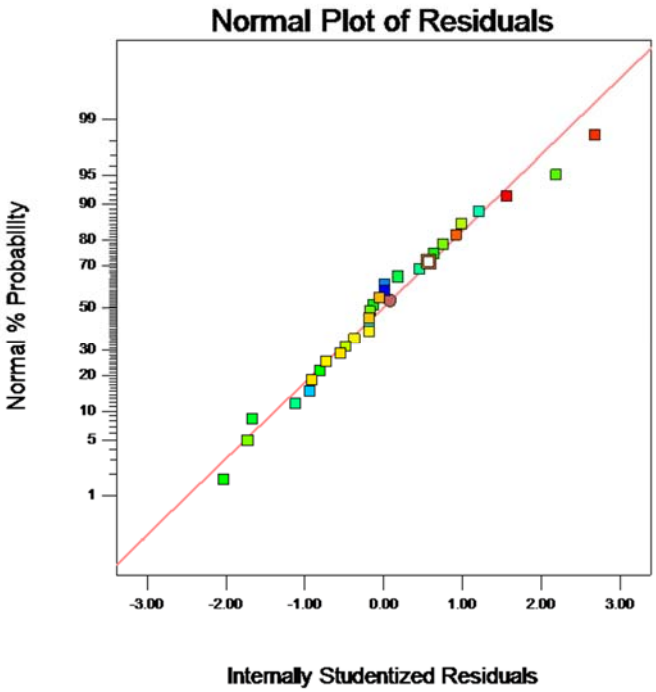

Fig. 2. Normal probability plot for BO yield.

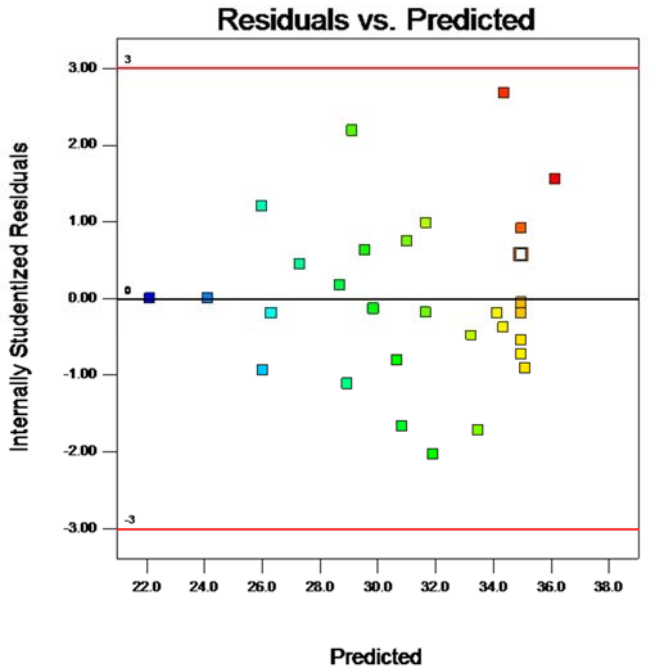

Fig. 3. Residual vs. predicted values for BO yield.

3.1.3 Response surface plots and optimization

Three dimensional response surface and contour plots for BO yield based on reaction temperature, reaction time, catalyst dosage, biomass/water mass ratio were plotted in Figs. 4-9. Since there are four factors in this study, each time the other two factors were fixed at their level "0" when plotting two factors. As illustrated in figures, all the curve shape of response surfaces are downwards convex, with a central point in the studied range, indicating that there is a maximum response for BO yield.

Fig. 4 shows the effect of reaction temperature and time on BO yield. The rate of the BO yield with temperature was greater than that of time, indicating that BO yield depended more on temperature than on time. This observation was consistent with findings reported in the literature (Chan et al., 2017; Gollakota et al., 2017; Jindal and Jha, 2016). The BO yield increased sharply as reaction temperature increased from 280 to 310 ºC, which was higher than 35.3 wt% when the temperature was between 305 and 309 ºC and time was between 15 and 17.3 min. When barley straw was treated at low temperature (at 260 ºC in run 25), the bond cleavage among different components could not be completely finished, at the same time reactions such as hydrolyzation and depolymerization leading to smaller molecules could not be finished. With increasing in temperature, the dehydration, decarboxylation, dehydroxylation reactions between macromolecules formed by initial reactions occurred and therefore BO containing various organic compounds (phenolics, organic acids, aromatic hydrocarbons) identified in Table 5, SR, gases were formed at relatively higher temperature. Further increase in temperature (>310 ºC), the yield of BO gradually decreased, accompanied by an increase in SR yield shown in Table 3. The reduction could be explained by the polymerization/condensation of phenols and their derivatives, which were unstable to form solid products at high temperatures, as evidenced by the decreased phenolics content in Fig. 10.

The effect of reaction temperature and catalyst dosage on BO yield is shown in Fig. 5. It showed that increase in both two independent variables enhanced the BO yield initially, but then slowly declined. There was an optimum point for temperature at around 308 ºC and catalyst dosage of 12.4 %. According to our previous study,

K_2CO_3 employed in a fixed concentration during HTL of barley straw changed reaction pathway where more phenolic compounds were formed in BO (Zhu et al., 2015b). Further increase in catalyst dosage at a fixed temperature gave insignificant influence on BO yield owing to the desired reactions such as decomposition/depolymerization were inhibited. Similar finding that optimal BO yield and energy recovery were obtained when a suitable catalyst amount was used during HTL of birch sawdust (Malins, 2017).

Fig. 6 illustrates the effect of reaction temperature and biomass/water ratio on BO yield. The BO yield increased with increasing temperature when it was below 305 ^{o}C at a fixed biomass/water ratio. Afterwards a slight decrease in BO yield was observed, which might be due to gasification of oily compounds or polymerization/condensation reactions mentioned above. It is evidenced that biomass-to-solvent ratio strongly affects BO and SR yield. When water was employed in HTL, it serves as both a solvent and hydrogen donor for hydrolyzing the molecules and therefore biomass/water ratio is a key parameter (Anastasakis and Ross, 2011; Cao et al., 2017). In Fig. 6, it can be observed that higher BO yield was reached utilizing appropriate biomass/water ratio (14.5-17%). Due to the role of water involved in the depolymerization reaction, much higher biomass/water ratio resulted in lower solubility of small molecular products or intermediates in water, and inhibited the formation of oily products.

The effect of reaction time and catalyst dosage on BO yield is depicted in Fig. 7. It can be observed that the effect of time was closely linked to catalyst dosage. More specifically, the BO yield showed no remarkable change with lower catalyst dosage (less than 8%). It increased as catalyst dosage increased from 8 to 13.6%, and then became nearly stationary. Maximum BO yield (35.3 wt%) was obtained when the catalyst content was between 11.2% and 12.3% and the time ranged from 15 to 18.3 min. Most importantly, when the catalyst dosage was above 10% and reaction time was longer than 15 min, both of two variables had no apparent impact on the BO yield, which was higher than 35 wt%. This implied that too short a reaction time was not enough for the BO formation, while too long may result in the SR formation as shown

in Table 3 or gas formation from cracking of liquid products as pointed by Xu et al. (Xu and Etcheverry, 2008).

Fig. 8 shows the effect of reaction time and biomass/water ratio on BO yield. As it is clear from this figure, higher BO yield was obtained at higher biomass/water ratio, which exceeded 35wt% when biomass/water ratio was above 16.2%. A further increase of this ratio caused insignificant changes in BO yield, the reasons of which have already been explained above in Fig. 6. While, the influence of reaction time on BO yield was relatively insignificant compared with the catalyst dosage and biomass/water ratio, as seen from Figs. 7 and 8. Therefore, it provided some guidance for the choice of important parameters in HTL of straw in continuous plant in the future. The effect of catalyst dosage and biomass/water ratio on BO yield is depicted in Fig. 9. It was observed that BO yield increased with biomass/water at a fixed catalyst dosage. This result indicated that the range of biomass/water ratio involved in this study was suitable for depolymerization reaction and BO formation. Higher BO yield appeared when the catalyst content was higher than 8.2% and biomass/water ratio was above 15%.

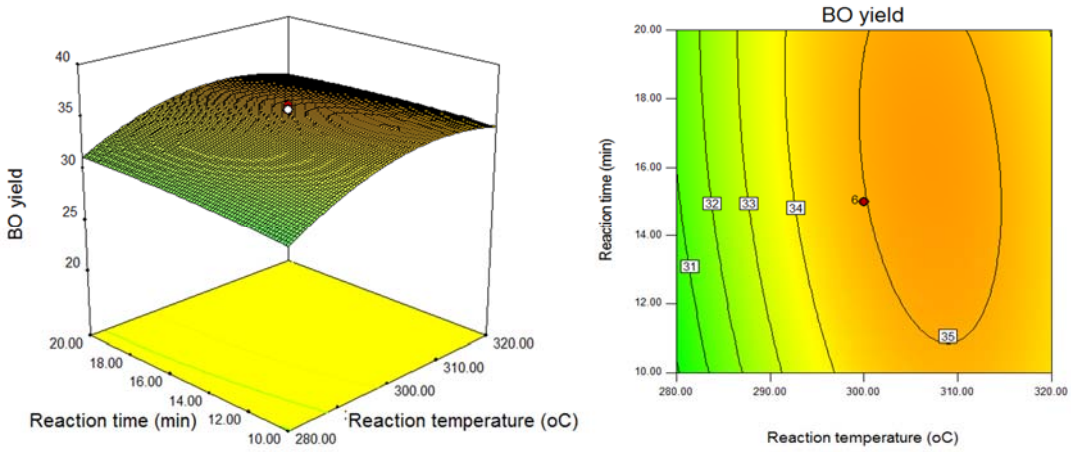

Fig. 4 The response surface (a) and contour plots (b) for BO yield as a function of temperature (°C) and reaction time (min).

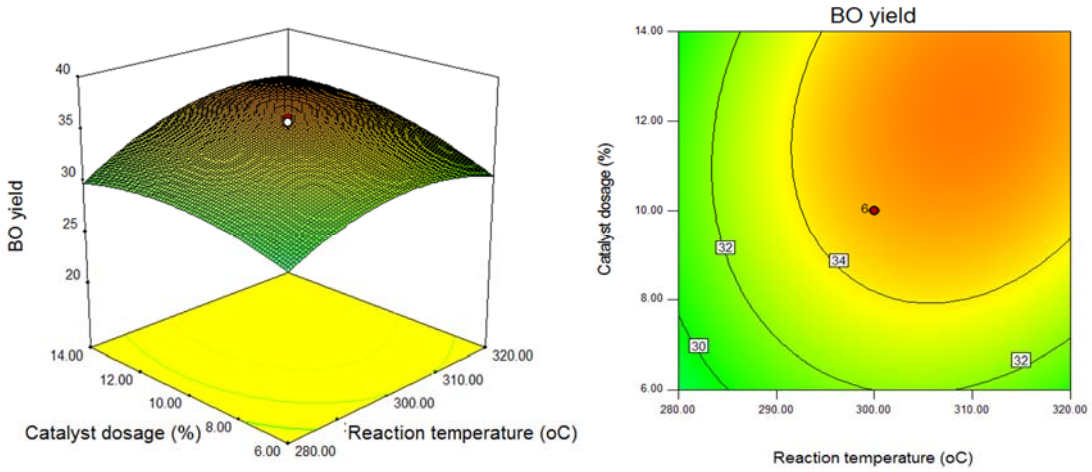

Fig. 5 The response surface (a) and contour plots (b) for BO yield as a function of temperature (ºC) and catalyst dosage (%).

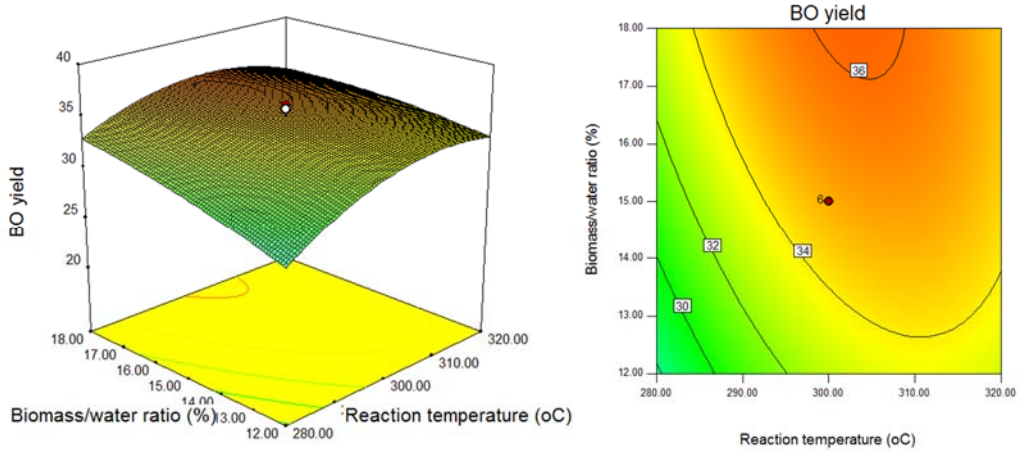

Fig. 6 The response surface (a) and contour plots (b) for BO yield as a function of temperature (ºC) and biomass/water ratio (%).

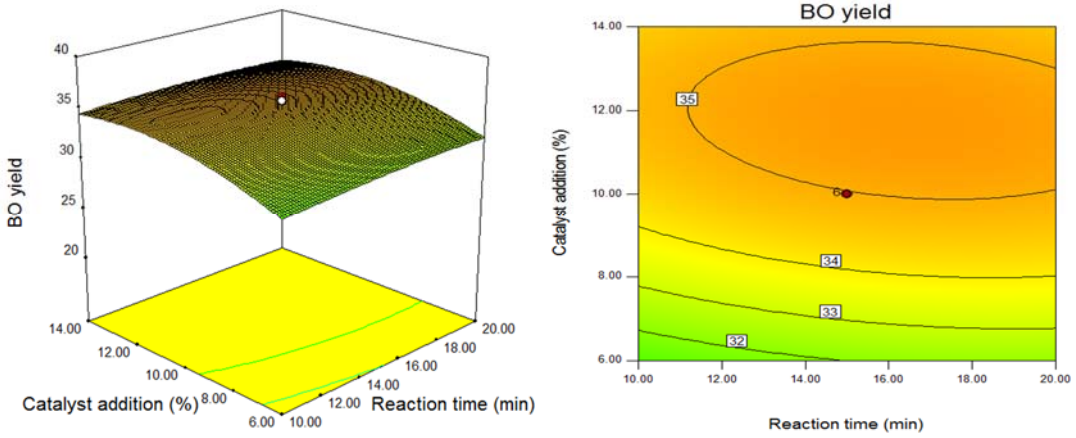

Fig. 7 The response surface (a) and contour plots (b) for BO yield as a function of reaction time (min) and catalyst dosage (%).

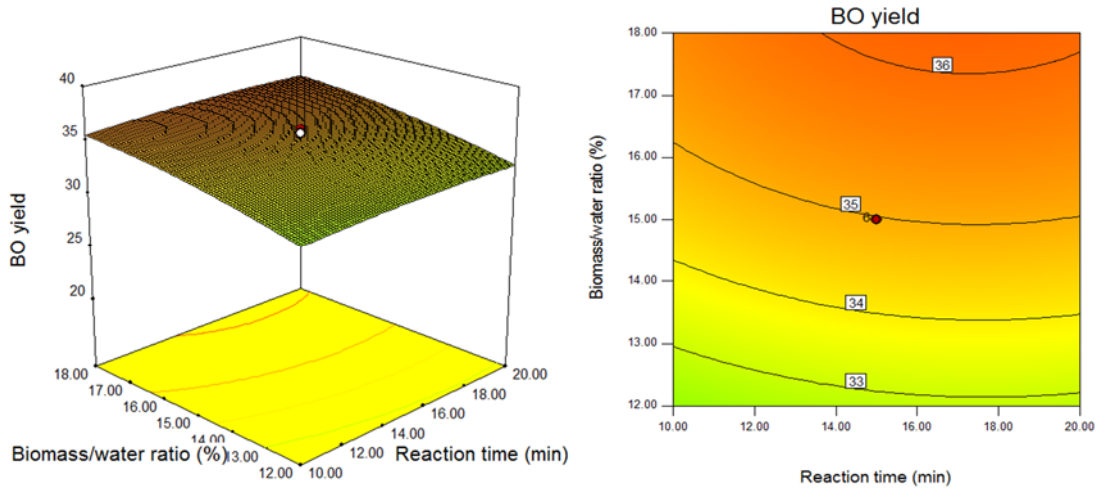

Fig. 8 The response surface (a) and contour plots (b) for BO yield as a function of reaction time (min) and biomass/water ratio (%).

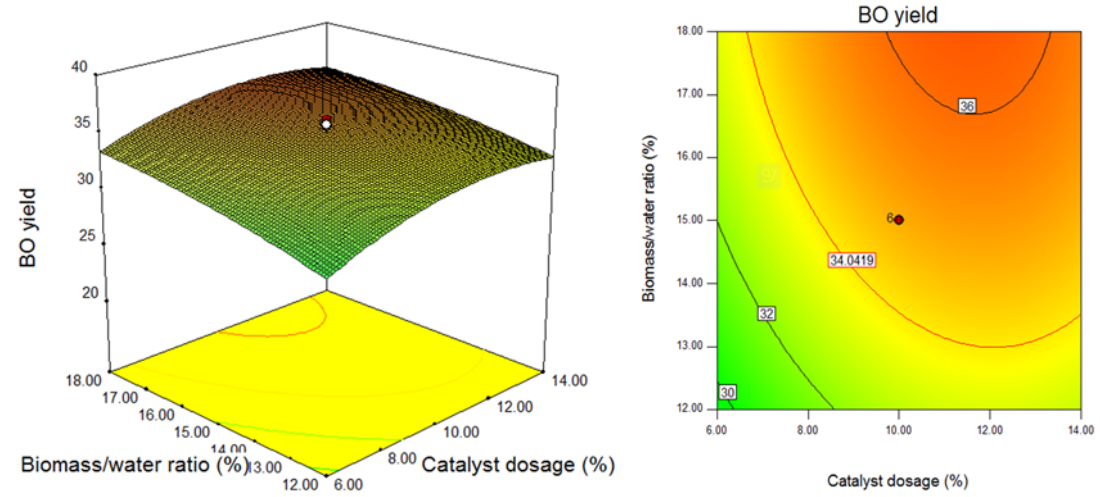

Fig. 9 The response surface (a) and contour plots (b) for BO yield as a function of catalyst dosage(%) and biomass/water ratio.

The optimum values of the process variables for the maximum BO yield are shown in Table 4. Higher biomass content was chosen for optimal utilization of waste, with a biomass/water ratio of 18.0 applied in optimization process. Confirmatory experiments were carried out three times under the predicted optimal condition in order to verify the predicted optimization result. It showed that the experimental BO yield closely agreed with model prediction value, with the error of 6.25. Therefore, RSM is a powerful tool for optimizing the operational conditions of BO production from barley straw.

Table 4 Optimum operating conditions, predicted and experimental BO yield

Optimum operating conditions				BO yield (wt%)		Error[a] (%)
Reaction temperature (°C)	Reaction time (min)	Catalyst dosage (%)	Biomass/water ratio	Predicted	Experimental	
304.8	15.5	11.7	18.0	36.46	38.72±0.36	6.25

[a] Error=(Experimental BO yield –Predicted BO yield)/ Predicted BO yield

3.2 Chemical compositions of BO

The elemental composition and HHV of BO are shown in Table 3. Herein BO obtained at 280 °C were not analyzed due to lower amount of BO yield, which is not anticipated in HTL process. According to Table 3, the carbon content was between 65.46% and 69.31%. Increasing the temperature led to a higher carbon content, while it showed no remarkable change on the hydrogen content (about 7%). In contrast, a prolonged reaction time or reduced catalyst dosage reduced carbon content in BO, which could be considered when optimizing HTL process. The HHV range from 26.80 and 30.17 MJ/kg.

BO obtained from barley straw is a very complex mixture. The chromatograms of BO are provided as supplementary material. Table 5 shows the organic compounds in BO at different operating conditions, and only the compounds with high content were listed here. Most components in BO were volatilized and detected due to the derivatization before GC/MS analysis. The relative contents of each compound determined by peak areas ratio were listed as well. Distribution of key groups of chemical compounds in BO obtained at different reaction conditions is presented in Fig. 10. As observed, the BO mainly consist of organic acids, phenols and their derivatives, aromatic hydrocarbons, ketones, aldehydes, alcohols and N-contained organic compounds. BO produced at lower temperature (300 °C) had higher phenolic compounds, lower long chain carboxylic acids and lower aromatics than that obtained at higher temperature (340 °C), while BO obtained from higher temperature was more complicated compare to lower temperature.

Table 5 Major organic compounds in the BO at different reaction conditions.

Peak	RT	Name of compound	Area (%)

	(min)		O-300	O-340
1	3.48	2-Hydroxypropanoic acid	2.95	
2	3.60	1-(3-methylbutyl)-2,3,4,6-tetrame thylbenzene	1.85	
3	4.02	Propanoic acid, 2-hydroxy-2-methyl	2.60	
4	4.18	Oenantholacton	1.08	
5	4.59	2,4-Hexadienoic acid, 1-methylethyl ester	1.12	
6	4.78	2-Methoxy phenol	2.19	
7	4.85	2,4-Dimethylphenol	1.58	0.82
8	5.16	Glycerol	1.41	
9	5.18	Phenol, 4-ethyl-2-methoxy-		0.67
10	5.44	1,3-Benzenediol	4.02	2.37
11	5.94	9,10-Anthracenedione, 1,4-dihydroxy-2,3-		1.79
12	5.96	3,5-Dimethylphenol	2.90	
13	5.96	.Alpha.-methylstilbene		2.09
14	6.01	2,6-Dimethoxyphenol	11.62	3.51
15	6.10	2,4-Dihydroxybutanoic acid	1.43	
16	6.39	Methylhydroquinone	3.58	
17	6.39	Fluorene		4.46
18	6.42	[1,1'-Biphenyl]-4-ol, 3,5-Bis(1,1-dimethylethyl)-		1.04
19	6.54	2,6-Dimethoxy-1-hydroxy-phenate butyl	4.07	
20	6.54	Noscapine		2.88
21	6.67	5,8-Dimethoxy-1,4-dimethyl-1,4-dihydro-2,3-quinoxalin edithione		0.97
22	6.70	1-Naphthalenol, 2-[(4-chlorophenyl)azo]	2.32	
23	6.83	2'-Hydroxypropiophenone		1.08
24	6.88	1,3-Dimethyl-6-ethyl-5-[(3-(2-acetamido-3-oxo-3-metho xy)propyl)indol-2-yl]-uracil		1.70
25	6.96	3,4-Dimethoybenzoic acid	2.13	1.59
26	7.08	1,3,5-Benzenetricarboxylic acid, trimethyl ester		0.83
27	7.4	9,10-Anthracenedione, 1,4-diamino-		0.65
28	7.48	(1E)-1-Phenyl-1-hepten-3-ol		1.49
29	7.74	Albomaculine		0.96
30	7.93	Oxazolidine-2,4-dione, 5-[4-(ethylmethylamino)phenyl]-		0.92
31	7.96	Ethanone,1-[4-(4-morpholylbenzylidenami	1.60	
32	7.99	Xylitol	1.11	
33	8.08	5,6,7,8-Tetrahydro-3-nitronaphthalen-2-ol-1-carboxylic acid, met		0.79
34	8.21	2,5-Cyclohexadien-1-one, 2,5-dimethyl-4-[(2,4,5-trimethylphenyl)]imi	5.11	
35	8.44	1,5-Diphenyl-3-styryl-2-pyrazolin	1.35	
36	8.44	Benzene, (2-methyl-1-propenyl)-		0.79
37	8.52	Tetradecanoic acid		4.26
38	8.53	2H,8H-Benzo[1,2-B:5,4-B']Dipyran-2-one, 5-methoxy-8,8-dimethyl- 10-(3-methyl-2-butenyl)-	5.20	

39	8.8	Albomaculine		1.50
40	9.49	Hexadecanoic acid	7.28	16.91
41	10.27	Oleic aicd	2.32	4.45
42	10.37	Octadecanoic acid	0.78	1.45
43	10.60	Benzyl ether	0.57	
44	10.90	Cyclopropaneoctanal, 2-octyl-		10.18
45	13.03	Azelaic acid		0.70
46	13.05	9,12,15-Octadecatrienoic acid	1.17	
Total			73.34	70.84

372

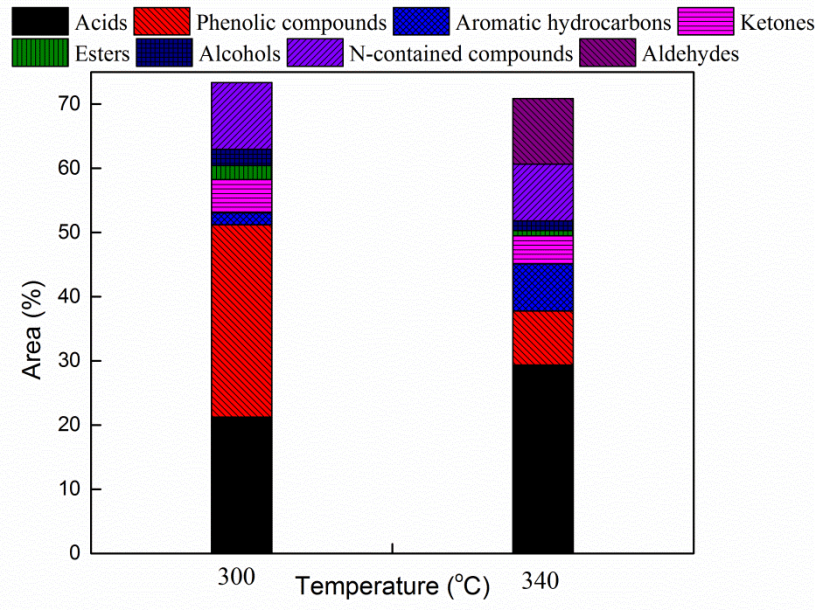

373

374 **Fig. 10** Distribution of key chemical compounds in BO obtained at different
375 reaction conditions. (left: 300 ºC, 15min, 10wt% catalyst and 15% biomass/water
376 ratio. right: 340 ºC, 15min, 10wt% catalyst and 15% biomass/water ratio.)

377 Phenols and their derivatives mainly contained 2,6-dimethoxyphenol,
378 1,3-benzenediol, methylhydroquinone, 3,5-dimethylphenol, 2-methoxy phenol,
379 2,4-dimethylphenol in BO produced at 300 ºC, accounting for 29.96% of detected
380 compounds. Higher phenolic compounds in BO makes it a promising material in the
381 applications of either as a phenol substitute in bio-phenolic resins or bio-fuel. While
382 their contents decreased or even disappeared at 340 ºC. Phenol derivatives could be
383 originated from cleavage of ether bonds or C-C linkage in lignin (Jindal and Jha,
384 2016), dehydration of furfurals during the degradation of cellulose or
385 dehydrogenation of aldehydes/acids (Nazem and Tavakoli, 2017). At higher
386 temperature, reactions such as hydrogenolysis, dehydrogenation and

dehydroaromatization may occur and therefore convert some phenolics to hydrocarbons (Cheng et al., 2017). This led to the decreased contents of phenolic compounds together with higher aromatic hydrocarbons content increasing from 1.85% at 300 ºC to 7.34% at 340 ºC. The presence of fluorine and benzene, (2-methyl-1-propenyl)- in BO at 340 ºC supported this statement.

Different types of organic acids were also detected in BO, most of which were long chain fatty acids. They mainly consist of hexadecanoic acid, oleic acid and octadecanoic acid, all of which increased when raising the temperature. Total organic acids accounted for 29.36% at 340 ºC. Short chain fatty acids such as 2-hydroxypropanoic acid and propanoic acid, 2-hydroxy-2-methyl can only be found in BO at 300 ºC. They were formed by the complex hydrolysis and dehydration reactions of the cellulose, hemicellulose and some extractives fraction in barley straw (Sun et al., 2011). BO obtained under this condition may have the potential to be converted into biodiesel. It should be noted that presence of organic acids would have an adverse effect in storage, transportation and catalytic upgrading (Mortensen et al., 2011).

Cyclic ketones, esters, and alcohols were observed in both BO. They were supposed to be derived from the decomposition of cellulose and hemicellulose components (Huber et al., 2006). As pointed by Chen et al., the ketones could transform between organic acids and alcohols due to their instability under HTL conditions(Chen et al., 2014). Table 5 also showed that BO contained small amounts of N-contained compounds, most probably due to the interaction between hydrolysis products from barley straw to form N-containing ring compounds via Mailard reaction (Kruse et al., 2007). Some of the identified compounds in BO are valuable for the chemical industry, which should be further treated according to its application.

4 Conclusions

A five-level CCD selected as a RSM for experiment design was employed to optimize the effect of influencing factors on BO production from HTL of barley straw. Four factors including reaction temperature (X_1),reaction time (X_2), catalyst dosage (X_3) and biomass/water ratio (X_4) were investigated. The ANOVA of quadratic model

revealed that BO yield was affected by reaction temperature, catalyst dosage and biomass/water ratio significantly. Besides, the influences of interaction of X_1X_3 and X_1X_4 were more significant. The optimum reaction conditions for the BO production were: a temperature of 304.8 ºC, a time of 15.5 min, a biomass/water ratio of 18% and a catalyst content of 11.7 %. The maximum BO yield was 38.72 wt% was obtained under optimum conditions. The experimental data are in good agreement with predicted values, indicating the accuracy of quadratic model for optimization of HTL of barley straw. GC/MS analysis showed that BO mainly contained organic acids, phenols and their derivatives, aromatic hydrocarbons, ketones, aldehydes, alcohols and N-contained organic compounds. The HHV of BO range from 26.80 and 30.17 MJ/kg, which has the potential to be used as a potential source of renewable fuel.

Acknowledgements

This research was financially supported by FLEXIfuel (DSF-BENMI grant no 10-094552). Zhe Zhu thanks the China Scholarship Council for the financial support.

References

Anastasakis K, Ross AB. Hydrothermal liquefaction of the brown macro-alga Laminaria Saccharina: Effect of reaction conditions on product distribution and composition. Bioresource Technology 2011; 102: 4876-4883.

Box GEP, Draper NR. Response Surfaces, Mixtures, and Ridge Analyses, 2nd Edition. New Jersey: John Wiley & Sons, Inc., 2007.

Cao L, Zhang C, Chen H, Tsang DCW, Luo G, Zhang S, et al. Hydrothermal liquefaction of agricultural and forestry wastes: state-of-the-art review and future prospects. Bioresource Technology 2017; 245: 1184-1193.

Chan YH, Quitain AT, Yusup S, Uemura Y, Sasaki M, Kida T. Optimization of hydrothermal liquefaction of palm kernel shell and consideration of supercritical carbon dioxide mediation effect. The Journal of Supercritical Fluids 2017.

Chen W-T, Zhang Y, Zhang J, Yu G, Schideman LC, Zhang P, et al. Hydrothermal liquefaction of mixed-culture algal biomass from wastewater treatment system into bio-crude oil. Bioresource Technology 2014; 152: 130-139.

Cheng S, Wei L, Julson J, Kharel PR, Cao Y, Gu Z. Catalytic liquefaction of pine sawdust for biofuel development on bifunctional Zn/HZSM-5 catalyst in supercritical ethanol. Journal of Analytical and Applied Pyrolysis 2017; 126: 257-266.

Déniel M, Haarlemmer G, Roubaud A, Weiss-Hortala E, Fages J. Bio-oil Production from Food Processing Residues: Improving the Bio-oil Yield and Quality by Aqueous Phase Recycle in

Hydrothermal Liquefaction of Blackcurrant (Ribes nigrum L.) Pomace. Energy & Fuels 2016; 30: 4895-4904.
Das O, Sarmah AK. Value added liquid products from waste biomass pyrolysis using pretreatments. Science of The Total Environment 2015; 538: 145-151.
Denmark S. StatBank Denmark, 2014.
Diamond WJ. Practical Experiment Design for Engineers and Scientists: Lifetime Learning Publications, 1981.
Eriksson L, Johansson E, Kettaneh-Wold N, Wikström C, Wold S. Design of Experiments Principles and Applications. Umeå, Sweden: Umetrics AB, 1996.
Gollakota ARK, Kishore N, Gu S. A review on hydrothermal liquefaction of biomass. Renewable and Sustainable Energy Reviews 2017.
Hassan SNAM, Ishak MAM, Ismail K. Optimizing the physical parameters to achieve maximum products from co-liquefaction using response surface methodology. Fuel 2017; 207: 102-108.
Hsieh D, Capareda S, Placido J. Batch Pyrolysis of Acid-Treated Rice Straw and Potential Products for Energy and Biofuel Production. Waste and Biomass Valorization 2015; 6: 417-424.
Hu Y, Feng S, Yuan Z, Xu C, Bassi A. Investigation of aqueous phase recycling for improving bio-crude oil yield in hydrothermal liquefaction of algae. Bioresource Technology 2017; 239: 151-159.
Huber GW, Iborra S, Corma A. Synthesis of transportation fuels from biomass: chemistry, catalysts, and engineering. Chemical Reviews 2006; 106: 4044-4098.
IEA. Energy Statistics, 2012.
Jindal MK, Jha MK. Effect of process parameters on hydrothermal liquefaction of waste furniture sawdust for bio-oil production. RSC Advances 2016; 6: 41772-41780.
Kruse A, Maniam P, Spieler F. Influence of Proteins on the Hydrothermal Gasification and Liquefaction of Biomass. 2. Model Compounds. Industrial & Engineering Chemistry Research 2007; 46: 87-96.
Kummamuru B. Global bioenergy statistics 2017, 2017.
Li X, Wang B, Wu S, Kong X, Fang Y, Liu J. Optimizing the Conditions for the Microwave-Assisted Pyrolysis of Cotton Stalk for Bio-Oil Production Using Response Surface Methodology. Waste and Biomass Valorization 2017; 8: 1361-1369.
Liu J, Zhuang Y, Li Y, Chen L, Guo J, Li D, et al. Optimizing the conditions for the microwave-assisted direct liquefaction of Ulva prolifera for bio-oil production using response surface methodology. Energy 2013; 60: 69-76.
Malins K. Production of bio-oil via hydrothermal liquefaction of birch sawdust. Energy Conversion and Management 2017; 144: 243-251.
Midgett JS, Stevens BE, Dassey AJ, Spivey JJ, Theegala CS. Assessing Feedstocks and Catalysts for Production of Bio-Oils from Hydrothermal Liquefaction. Waste and Biomass Valorization 2012; 3: 259-268.
Mortensen PM, Grunwaldt JD, Jensen PA, Knudsen KG, Jensen AD. A review of catalytic upgrading of bio-oil to engine fuels. Applied Catalysis A: General 2011; 407: 1-19.
Nazem MA, Tavakoli O. Bio-oil production from refinery oily sludge using hydrothermal liquefaction technology. The Journal of Supercritical Fluids 2017; 127: 33-40.
Parsa M, Jalilzadeh H, Pazoki M, Ghasemzadeh R, Abduli M. Hydrothermal liquefaction of Gracilaria gracilis and Cladophora glomerata macro-algae for biocrude production. Bioresource Technology 2018; 250: 26-34.

Patel B, Guo M, Chong C, Sarudin SHM, Hellgardt K. Hydrothermal upgrading of algae paste: Inorganics and recycling potential in the aqueous phase. Science of The Total Environment 2016; 568: 489-497.

Sander B. Properties of Danish biofuels and the requirements for power production. Biomass and Bioenergy 1997; 12: 177-183.

Suárez-Iglesias O, Urrea JL, Oulego P, Collado S, Díaz M. Valuable compounds fromsewage sludge by thermal hydrolysis and wet oxidation. A review. Science of the Total Environment 2017; 584-585: 921-934.

Sun P, Heng M, Sun S-H, Chen J. Analysis of liquid and solid products from liquefaction of paulownia in hot-compressed water. Energy Conversion and Management 2011; 52: 924-933.

Toor SS, Rosendahl L, Rudolf A. Hydrothermal liquefaction of biomass: A review of subcritical water technologies. Energy 2011; 36: 2328-2342.

Xiu S, Shahbazi A. Bio-oil production and upgrading research: A review. Renewable and Sustainable Energy Reviews 2012; 16: 4406-4414.

Xu C, Etcheverry T. Hydro-liquefaction of woody biomass in sub- and super-critical ethanol with iron-based catalysts. Fuel 2008; 87: 335-345.

Xu L, Jiang Y, Wang L. Thermal decomposition of rape straw: Pyrolysis modeling and kinetic study via particle swarm optimization. Energy Conversion and Management 2017; 146: 124-133.

Younas R, Hao S, Zhang L, Zhang S. Hydrothermal liquefaction of rice straw with NiO nanocatalyst for bio-oil production. Renewable Energy 2017; 113: 532-545.

Yu KL, Lau BF, Show PL, Ong HC, Ling TC, Chen W-H, et al. Recent developments on algal biochar production and characterization. Bioresource Technology 2017.

Zhang B, von Keitz M, Valentas K. Thermochemical liquefaction of high-diversity grassland perennials. Journal of Analytical and Applied Pyrolysis 2009; 84: 18-24.

Zhu Z, Rosendahl L, Toor SS, Yu D, Chen G. Hydrothermal liquefaction of barley straw to bio-crude oil: Effects of reaction temperature and aqueous phase recirculation. Applied Energy 2015a; 137: 183-192.

Zhu Z, Toor S, Rosendahl L, Yu D, Chen G. Influence of alkali catalyst on product yield and properties via hydrothermal liquefaction of barley straw. Energy 2015b; 80: 284-292.

Zhu Z, Toor SS, Rosendahl L, Chen G. Analysis of product distribution and characteristics in hydrothermal liquefaction of barley straw in sub- and supercritical water. Environmental Progress & Sustainable Energy 2014; 33: 737-743.